Available online at www.sciencedirect.com
SCIENCE DIRECT®

ELSEVIER

Ocean Engineering 31 (2004) 1129–1146

OCEAN ENGINEERING

www.elsevier.com/locate/oceaneng

Sound radiation from a liquid-filled underwater spherical acoustic lens with an internal eccentric baffled spherical piston

Seyyed M. Hasheminejad *, Mahdi Azarpeyvand

Department of Mechanical Engineering, Iran University of Science and Technology, Narmak, Tehran 16844, Iran

Received 4 June 2003; accepted 1 October 2003

Abstract

An exact study on reradiation of an acoustic field due to radial/axial vibrations of a baffled spherical piston, while eccentrically positioned within a fluid-filled thin spherical elastic shell, into an external fluid medium is presented. This configuration, which is a realistic idealization of a liquid-filled spherical acoustic lens with focal point inside the lens when used as a sound projector, is of practical importance with multitude of possible applications in ocean engineering and underwater acoustics. The formulation utilizes the appropriate wave field expansions along with the translational addition theorems for spherical wave functions to develop a closed-form solution in form of infinite series. Numerical results reveal that in addition to frequency, cap angle, radiator position (eccentricity), cap surface velocity distribution, and dynamics of the elastic shell can be of significance in sound radiation.

Keywords: Acoustic lens; Spherical piston; Elastic shell; Addition theorem; Cap angle

1. Introduction

Acoustic scattering (radiation) by pairs of interacting spherical bodies is essentially a multiple scattering problem that has received substantial attention in the acoustics literature (Bostrom, 1980; Gaunaurd et al., 1995; Gabrielli and Mercier-Finidori, 2001; Huang and Gaunaurd, 1997a; Thompson, 1977, 1983). Similarly,

* Corresponding author. Tel.: +98-21-739-12936; fax: +98-21-745-4050/1143.
E-mail address: hashemi@iust.ac.ir (S.M. Hasheminejad).

0029-8018/$ - see front matter
doi:10.1016/j.oceaneng.2003.10.010

the studies of acoustic scatterers (radiators) near boundaries have taken extensive consideration (Gaunaurd and Huang, 1995, 1996; Hasheminejad, 2001; Huang and Gaunaurd, 1997b). On the other hand, the solutions of acoustic wave radiation problems in multiply connected domains bounded by eccentric spherical surfaces seem to be quite sparse. Roumeliotis et al. (1991) and Roumeliotis and Kanellopoulos (1992) employed a special shape perturbation method to derive analytical expressions for the acoustic resonance frequency shifts in a hard- (soft-) walled spherical cavity, caused by introduction of an eccentric small inner sphere. The more closely related problem of acoustic radiation from a spherical source embedded eccentrically within a fluid sphere and vibrating with an arbitrary, axisymmetric, time-harmonic velocity distribution is analyzed by Thompson (1973). In more recent papers (Lease and Thompson, 1991a, b), this analysis is generalized for a number of non-axisymmetric spherical sources within a fluid sphere. Just recently, an exact study on radiation of sound from a shell-encapsulated (eccentric) spherical source, which is undergoing harmonic modal surface vibrations, is offered by Hasheminejad and Azarpeyvand (in press).

The acoustic radiation from pistons placed on baffles has extensively been considered in the literature for various piston and baffle geometries (i.e. planes, spheres, cylinders, and spheroids). The self-radiation impedance for the classic problem of a radially (axially) vibrating piston on a rigid sphere is presented by Skudrzyk (1971) and Morse (1981). The mutual acoustic impedance of pistons on a sphere and a cylinder are analyzed by Sherman (1959) and Greenspon and Sherman (1964), respectively. Likewise, the acoustic radiation impedance of curved vibrating caps and rings located on hard baffles of prolate and oblate spheroidal obstacles are formulated by Van Buren (1971) and Baier (1972). Just lately, Boisvert and Van Buren, 2002 studied the self and mutual radiation impedances for rectangular piston sources vibrating on a rigid prolate spheroidal baffle.

A small spherical source freely suspended inside a fluid-filled spherical elastic shell, which is itself submerged in an unbounded acoustic field, may be regarded as a sensible model for a spherical acoustic lens when used as a sound projector rather than a receiver (Belcher, 1993; Makarchenko et al., 1989). A very simple model of the spherical acoustic lens used as a receiver was originally analyzed by Boyles (1965). In this analysis, the author considered a plane wave to be incident upon the lens and solved for the pressure field at any point within it, under the assumption that the actual sensor (hydrophone) was infinitesimally small so that it did not perturb the field. The same author has also published an analysis of the lens as a sound projector (Boyles, 1969) where he assumed that the actual source was a point source located at the focal point of a perfectly focusing (Luneburg) lens. A primitive model of the spherical acoustic lens used as a sound projector is examined by Thompson (1973). A more realistic model is analyzed by Hasheminejad and Azarpeyvand (in press). An analytical study on reradiation of acoustic signals (transient pulse) from a centrosymmetrical internal point source through a fluid-filled spherical elastic shell into an external fluid medium is offered by Poddubnyak et al. (1985) and Menton and Magrab (1973). The principal objective of current paper is to study the effect of cap angle (effective radiation area) on acoustic radiation from a fluid-filled spherical acoustic lens containing an internal eccentric baffled spherical piston. Therefore, the present work is in fact a realistic extension of the basic models presented by Thompson (1973) and Hasheminejad and Azarpeyvand (in press) for the case when the internal source is partially baffled (i.e. it is not wholly vibrating).

2. Formulation

The problem considered here is that of computing acoustic radiation from a spherical elastic shell with an internal eccentric baffled spherical piston that is radially/axially vibrating with a time-harmonic, axisymmetric, and arbitrary velocity. The geometry and the coordinate systems used are depicted in Fig. 1. The source sphere is considered to be displaced a distance r_0 from center of the shell along the z-axis as shown in the figure. The origins O_1 and O_2 of the two spherical coordinate systems $(r_1, \theta_1, \vartheta_1)$ and $(r_2, \theta_2, \vartheta_2)$ are place at the center of the radiator and the shell, respectively. Both coordinate systems have the same azimuthal coordinate ϑ, which is not shown in the figure. The direct distance between the center of the radiator and the receiver (field point) is r_1; the distance between the center of the shell and the receiver (field point) is r_2. The problem can be analyzed by means of the standard methods of theoretical acoustics. The fluid is assumed to be inviscid and ideal compressible. Thus, one may start with the familiar wave equation in an ideal compressible fluid (Pierce, 1991):

$$\frac{\partial^2 p}{\partial t^2} - c^2 \nabla^2 p = 0 \tag{1}$$

where p is the acoustic pressure, c is the ideal speed of sound evaluated at ambient conditions, and ∇^2 is the Laplacian operator. As the spherical source is assumed to undergo time-harmonic surface oscillations with frequency ω, we expect solutions

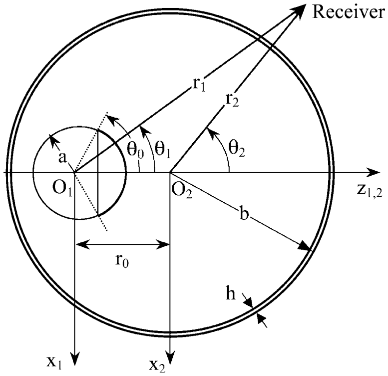

Fig. 1. Problem geometry.

of the form (Pierce, 1991)

$$p(r,\theta,\vartheta,t) = \mathrm{Re}\left[\bar{p}(r,\theta,\vartheta,\omega)e^{-i\omega t}\right] \tag{2}$$

where Re indicates the real part of a complex number, and quantity $\bar{p}(r,\theta,\vartheta,\omega)$ may be complex. Substitution of above presumption into (1) yields a Helmholtz-type equation:

$$(\nabla^2 + k^2)p = 0 \tag{3}$$

where $k = \omega/c$ is the acoustic wave number, and we have assumed harmonic time variations throughout with $e^{-i\omega t}$ dependence and also the over-bar notation suppressed for simplicity.

The spherical source is supposed to be rigid except for a cap region ($0 \le \theta \le \theta_0$), which is vibrating radially (axially) with a prescribed velocity $U^{(0)}$ ($U^{(1)}$). The cap velocity can be expressed as a linear combination of spherical modes in the form of infinite series (Skudrzyk, 1971)

$$\begin{aligned} u^{(0)}(\omega) &= \sum_{n=0}^{\infty} U_n^{(0)}(\omega)P_n(\cos\theta_1) = \begin{cases} U^{(0)}(\omega)P_0(\cos\theta_1) & 0 \le \theta_1 \le \theta_0 \\ 0 & \theta_0 \le \theta_1 \le \pi \end{cases} \\ u^{(1)}(\omega) &= \sum_{n=0}^{\infty} U_n^{(1)}(\omega)P_n(\cos\theta_1) = \begin{cases} U^{(1)}(\omega)P_1(\cos\theta_1) & 0 \le \theta_1 \le \theta_0 \\ 0 & \theta_0 \le \theta_1 \le \pi \end{cases} \end{aligned} \tag{4}$$

where $U_n^{(0)}(\omega)$ and $U_n^{(1)}(\omega)$ are the modal coefficients of radial and axial velocity distributions, respectively. These coefficients can readily be determined after multiplying both sides of (4) by $P_m(\eta_1 = \cos\theta_1)$, $(m = 0, 1, 2, \ldots)$, integrating over $d\eta_1$, and subsequently applying the orthogonality property of the Legendre functions. As a result, we obtain

$$\begin{aligned} U_n^{(0)}(\omega) &= \left(n + \frac{1}{2}\right)U^{(0)}(\omega)\int_{\eta_0}^{1} P_n(\eta_1)\mathrm{d}\eta_1 = \frac{1}{2}[P_{n-1}(\eta_0) - P_{n+1}(\eta_0)]U^{(0)}(\omega) \\ U_n^{(1)}(\omega) &= \left(n + \frac{1}{2}\right)U^{(1)}(\omega)\int_{\eta_0}^{1} \eta_1 \cdot P_n(\eta_1)\mathrm{d}\eta_1 \\ &= \frac{1}{2}\left\{\frac{n+1}{2n+3}[P_n(\eta_0) - P_{n+2}(\eta_0)] + \frac{n}{2n-1}[P_{n-2}(\eta_0) - P_n(\eta_0)]\right\}U^{(1)}(\omega) \end{aligned} \tag{5}$$

where the integrations are performed by making use of the following well-known relations (Skudrzyk, 1971):

$$\begin{aligned} &(2n+1)\int_{\eta_0}^{1} P_n(\eta)\mathrm{d}\eta = P_{n-1}(\eta_0) - P_{n+1}(\eta_0) \\ &(2n+1)\eta P_n(\eta) = (n+1)P_{n+1}(\eta) + nP_{n-1}(\eta) \end{aligned} \tag{6}$$

The fluid in the interior of the spherical shell is denoted as region I, while the outer medium is denoted as region II. In region I, the possibility of both incoming and outgoing (standing) waves exists while in region II, only outgoing waves are possible. The solution of the Helmholtz equation for the acoustic pressures can be obtained by means of spherical Hankel functions for the exterior region and spherical Hankel functions of the first and second kind for the interior region. In addition, due to the assumed velocity distribution, the acoustic pressure must be symmetric about the z-axis, i.e. independent of the azimuthal coordinate ϑ. Accordingly, the acoustic pressure inside the fluid-filled spherical shell may be represented by

$$p^{\mathrm{I}}(r_1,\theta_1,\omega)=\sum_{n=0}^{\infty}\gamma_n\left[a_n(\omega)h_n^{(1)}(kr_1)+b_n(\omega)h_n^{(2)}(kr_1)\right]P_n(\cos\theta_1) \tag{7}$$

where $\gamma_n=i^n(2n+1)$, $k=\omega/c$ is the acoustic wave number in fluid medium I, $h_n^{(1)}$ and $h_n^{(2)}$ are spherical Hankel functions of first and second kind, respectively (Abramowitz and Stegun, 1965), P_n is Legendre polynomial, and $a_n(\omega)$, $b_n(\omega)$ are unknown modal coefficients. Similarly, noting that the external fluid medium is unbounded and keeping in mind the radiation condition, the solution can be expressed as a linear combination of outgoing spherical waves as follows:

$$p^{\mathrm{II}}(r_2,\theta_2,\omega)=\sum_{n=0}^{\infty}\gamma_n c_n(\omega)h_n^{(1)}(k^*r_2)P_n(\cos\theta_2) \tag{8}$$

where $k^*=\omega/c^*$ is the acoustic wave number in fluid medium II, and the asterisks refer to the acoustic parameters in the outer fluid medium.

The equations of motion for a closed spherical elastic shell, including both membrane (extensional) and flexural (inextensional) effects, are presented by Junger and Feit (1986). The general displacements of the spherical shell are normally expressed in terms of the shell's midsurface deflections. Considering only the nontorsional axisymmetric motions, the midsurface radial $W(\omega,\theta_2)$ and tangential $V(\omega,\theta_2)$ displacements may be expanded in spherical harmonics as (Junger and Feit, 1986)

$$\begin{aligned}W(\omega,\theta_2)&=\sum_{n=0}^{\infty}W_n(\omega)P_n(\cos\theta_2)\\ V(\omega,\theta_2)&=\sum_{n=0}^{\infty}V_n(\omega)P_n^1(\cos\theta_2)\end{aligned} \tag{9}$$

where $P_n^1(\;)$ is Legendre function of first order (Abramowitz and Stegun, 1965). The equations of shell motion are satisfied if the modal coefficients $W_n(\omega)$ and $V_n(\omega)$ satisfy the equations (Junger and Feit, 1986)

$$\begin{aligned}&\left[\Omega^2-(1+\beta^2)(\upsilon+\lambda_n-1)\right]V_n(\omega)-\left[\beta^2(\upsilon+\lambda_n-1)+(1+\upsilon)\right]W_n(\omega)=0\\ &-\lambda_n\left[\beta^2(\upsilon+\lambda_n-1)+(1+\upsilon)\right]V_n(\omega)+\left[\Omega^2-2(1+\upsilon)-\beta^2\lambda_n(\upsilon+\lambda_n-1)\right]\\ &\qquad\times W_n(\omega)=-\frac{b^2(1-\upsilon^2)}{Eh}\Delta p_n(\omega)\end{aligned} \tag{10}$$

where $\beta^2=h^2/12b^2$, $\lambda_n=n(n+1)$, $\Omega=\omega b/c_p$ is a nondimensional frequency parameter, $c_p^2 = E/(1-\upsilon^2)\rho_s$ is the phase velocity of compressional wave in the elastic shell, ρ_s is the solid material density, h is the shell thickness, E is the modulus of elasticity and υ is the Poisson ratio. Furthermore, $\Delta p_n = p_n^{\mathrm{I}} - p_n^{\mathrm{II}}$ is modal component of the acoustic pressure differential at the shell's surface that can be expressed in the coordinate system of the elastic shell (r_2, θ_2) through application of the classical form of translational addition theorem for bi-spherical coordinates (Ivanov, 1970):

$$\left\{ \begin{array}{c} h_n^{(1)}(kr_1) \\ h_n^{(2)}(kr_1) \end{array} \right\} \cdot P_n(\cos\theta_1) = \sum_{n=0}^{\infty} R_{mn}(kr_0) \left\{ \begin{array}{c} h_m^{(1)}(kr_2) \\ h_m^{(2)}(kr_2) \end{array} \right\} \cdot P_m(\cos\theta_2) \tag{11}$$

where

$$R_{mn}(kr_0) = i^{m-n} \sum_{\mu=|m-n|}^{m+n} \varepsilon_\mu (-i)^\mu (2\mu+1) b_m^{n\mu} j_\mu(kr_0) \tag{12}$$

in which $\varepsilon_\mu = 1$ ($\varepsilon_\mu = (-1)^\mu$) when O_1 is on the left (right) hand side of O_2 (Fig. 1), $b_m^{n\mu} = (n\mu 00|m0)^2$, and Clebsch–Gordan coefficients are defined, with $q = (\mu + n + m)/2$ and $2q$ being even, as

$$\begin{aligned} (n\mu 00|m0) = & \frac{(-1)^{m+q} q!}{(q-n)!(q-\mu)!(q-m)!} \\ & \times \sqrt{\frac{(2m+1)}{(2q+1)!}(2q-2n)!(2q-2\mu)!(2q-2m)!} \end{aligned} \tag{13}$$

and when $2q$ is odd, $(n\mu 00|m0) = 0$. Subsequently, incorporation of (11) in (8), along with (7), allows us to express the pressure differential at the shell's surface as

$$\Delta p(\theta_2, \omega) = \sum_{n=0}^{\infty} \Delta p_n(\omega) P_n(\cos\theta_2) \tag{14}$$

where

$$\begin{aligned} \Delta p_n(\omega) = & \gamma_n \sum_{m=0}^{\infty} \left[a_m(\omega)\, h_n^{(1)}(kb_-) + b_m(\omega)\, h_n^{(2)}(kb_-) \right] R_{mn}(kr_0) \\ & - \gamma_n\, c_n(\omega)\, h_n^{(1)}(k^* b_+) \end{aligned} \tag{15}$$

in which $b_\pm = b \pm h/2$ (Fig. 1), and the appropriate change of indices are performed to enable factoring out the angular function $P_n(\ )$.

The unknown modal coefficients, $a_n(\omega)$, $b_n(\omega)$, and $c_n(\omega)$, must be determined by imposing the suitable boundary conditions. Accordingly, the continuity of normal velocities at the surface of the source requires that

$$\frac{1}{i\omega\rho} \cdot \frac{\partial p^{\mathrm{I}}(r_1, \theta_1, \omega)}{\partial r_1} \Bigg]_{r_1=a} = \sum_{n=0}^{\infty} \left\{ \begin{array}{c} U_n^{(0)}(\omega) \\ U_n^{(1)}(\omega) \end{array} \right\} P_n(\cos\theta_1) \tag{16}$$

where ρ is the fluid density in (inner) region I. Similarly, the continuity of normal velocities at the inner and outer surfaces of the spherical shell implies that

$$(-i\omega)W(\theta_2,\omega) = \frac{1}{i\omega\rho}\cdot\frac{\partial p^{\mathrm{I}}(r_2,\theta_2,\omega)}{\partial r_2}\bigg]_{r_2=b_-} = \frac{1}{i\omega\rho^*}\cdot\frac{\partial p^{\mathrm{II}}(r_2,\theta_2,\omega)}{\partial r_2}\bigg]_{r_2=b_+} \tag{17}$$

Incorporating (5) in the boundary conditions (16), we obtain, for the $n \geq 0$ modes at $r_1 = a$,

$$\frac{\gamma_n}{i\rho c}\left[a_n(\omega)h_n^{(1)'}(ka) + b_n(\omega)h_n^{(2)'}(ka)\right] = \begin{cases} U_n^{(0)}(\omega) & \text{Radial Vibrations} \\ U_n^{(1)}(\omega) & \text{Axial Vibrations} \end{cases} \tag{18}$$

Making use of the series expansions (7) and (8), and also the addition theorems (11) in the boundary conditions (17) yield

$$\begin{aligned} &\omega W_n(\omega) - \frac{\gamma_n}{\rho c}\sum_{m=0}^{\infty}\left[a_m(\omega)\ h_n^{(1)'}(kb_-) + b_m(\omega)\ h_n^{(2)'}(kb_-)\right]R_{mn}(kr_0) = 0 \\ &\omega W_n(\omega) - \frac{\gamma_n}{\rho^* c^*}h_n^{(1)'}(k^* b_+)c_n(\omega) = 0 \end{aligned} \tag{19}$$

where the prime symbol indicates the derivative with respect to the argument, and the modal components of shell's midsurface displacements, $W_n(\omega)$ and $V_n(\omega)$, satisfy (10). Subsequently, the unknown coefficients $a_n(\omega)$, $b_n(\omega)$, and $c_n(\omega)$ may readily be computed by solving the linear system of equations (18), (19) and (10).

Now, from (8), the radiated acoustic pressure in the far-field may be written as

$$p^{\mathrm{II}}(r_\infty,\theta_2,\omega) = \left(\frac{e^{ik^* r_\infty}}{ik^* r_\infty}\right)\sum_{n=0}^{\infty}(2n+1)\ c_n(\omega)P_n(\cos\theta_2) \tag{20}$$

where we have used the following asymptotic expansion for the spherical Hankel function (Abramowitz and Stegun, 1965):

$$h_n^{(1)}(k^* r_2)\Big]_{r_2\to r_\infty} \approx i^{-(n+1)}\frac{e^{ik^* r_\infty}}{k^* r_\infty} \tag{21}$$

Subsequently, the relative on-axis forward radiated far-field pressure, or the form function amplitude, may be defined as

$$f_\infty(\omega, r_0) = \left|\frac{p^{\mathrm{II}}(r_\infty,\theta_2=0,\omega)}{p^{\mathrm{II}}(r_\infty,\theta_2=0,\omega)]_{r_0=0}}\right| \tag{22}$$

where we note that the normalization is performed with respect to the case when the source is positioned exactly at the center of the shell. This completes the necessary background required for the exact acoustic analysis of the problem. Next, we consider some numerical examples.

3. Numerical results and discussion

In order to illustrate the nature and general behaviour of the solution, we consider a numerical example in this section. Realizing the large number of parameters involved here, no attempt is made to exhaustively evaluate the effect of varying each of them. The intent of the collection of data presented here is merely to illustrate the kinds of results to be expected from some representative and physically realistic choices of values for these parameters. From these data, some trends are noted and general conclusions made about the relative importance of certain parameters. Correspondingly, noting the crowd of parameters that enter into the final expressions and keeping in view the availability of numerical data, we shall confine our attention to a particular model. The surrounding ambient fluid is assumed to be water at atmospheric pressure and 300 K. The elastic shell is taken to be a 3% stainless steel shell of radius $b = 10$ cm, and thickness $h = 0.03b = 0.3$ cm. The piston is set on a rigid spherical baffle of radius $a = 0.01b = 0.1$ cm. The interior fluid is selected as 3M Company "Fluorinert" chemical FC-72 (available: http://www.mmm.com; 3M FC). The numerical values for the input parameters, which are used in the calculations, are summarized in Table 1. A MATLAB code was constructed for treating boundary conditions, to determine the unknown modal coefficients, and to compute the relevant acoustic quantities as functions of the nondimensional frequency $kb_e = \omega b_e/c$ [where $b_e = b\sin(\theta_0/2)$ is the effective piston radius; see Skudrzyk, 1971], and distance parameter r_0/b for selected cap angles θ_0. Accurate computations for derivatives of spherical Bessel functions were accomplished by utilizing (10.1.19) and (10.1.22) in the handbook by Abramowitz and Stegun (1965). The computations were performed on a Pentium IV personal computer with a truncation constant of $N = 30$ to assure convergence in the high frequency range, and also in case of close proximity of the source to the shell boundary (high eccentricity).

The far-field on-axis radiated pressure for the case of a radially/axially vibrating baffled spherical piston that is located at the center of the shell is primarily examined. Fig. 2 displays the effects of the nondimensional frequency, kb_e, and the cap angle, θ_0, on the on-axis far-field pressure magnitude, $|p^{\mathrm{II}}(r_\infty, \theta_2 = 0, \omega)|_{r_0=0}$. In addition, to further examine the shell dynamic interaction effects, we have

Table 1
Input parameter values

Fluid properties parameter	Numerical value	Elastic shell parameter	Numerical value
Pressure (bar)	1.00	E (dyn/cm^2)	2.15×10^{12}
Temperature (K)	300	h (cm)	0.3
c (cm/s)	5.12×10^4	ν	0.283
ρ (g/cm^3)	1.68	ρ_s (g/cm^3)	7.8
c^* (cm/s)	1.49×10^5	b (cm)	10
ρ^* (g/cm^3)	0.997	a (cm)	0.1

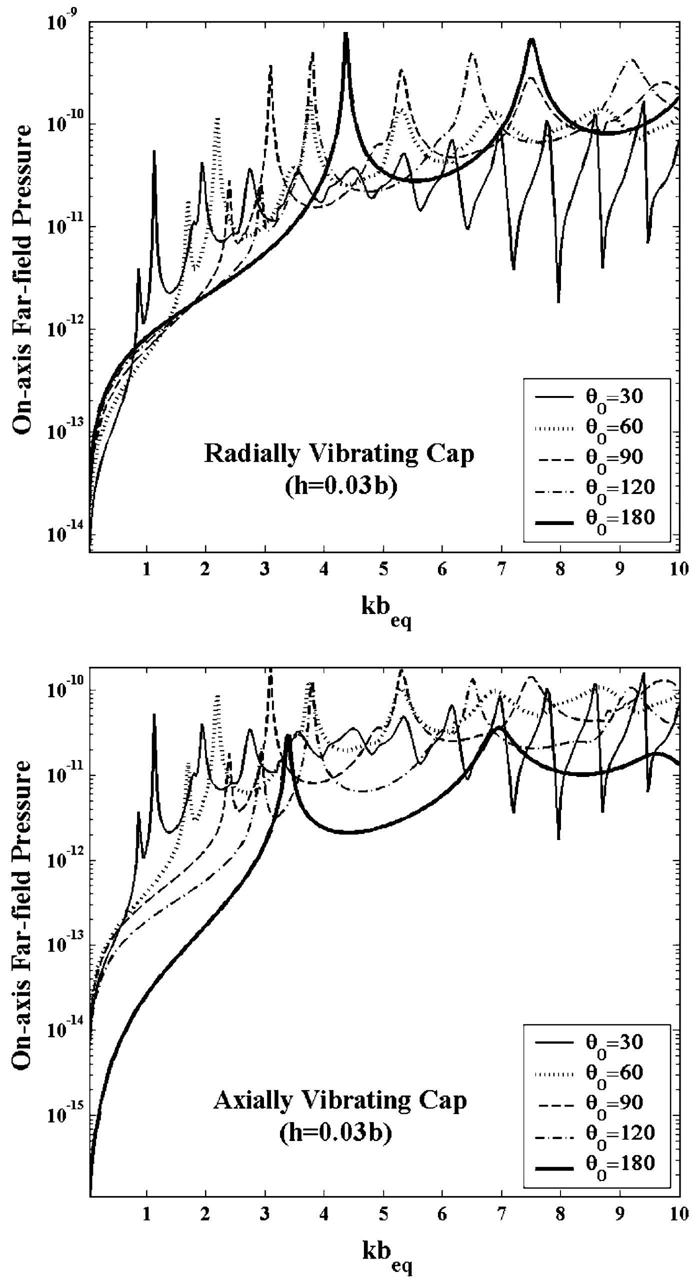

Fig. 2. The change in the on-axis far-field pressure magnitude with the nondimensional frequency for the radially/axially vibrating piston positioned in the center of the elastic shell for selected the cap angles.

presented the on-axis far-field pressure magnitude in absence of the shell in Fig. 3. Comparison of these figures leads to following observations. As the nondimen-

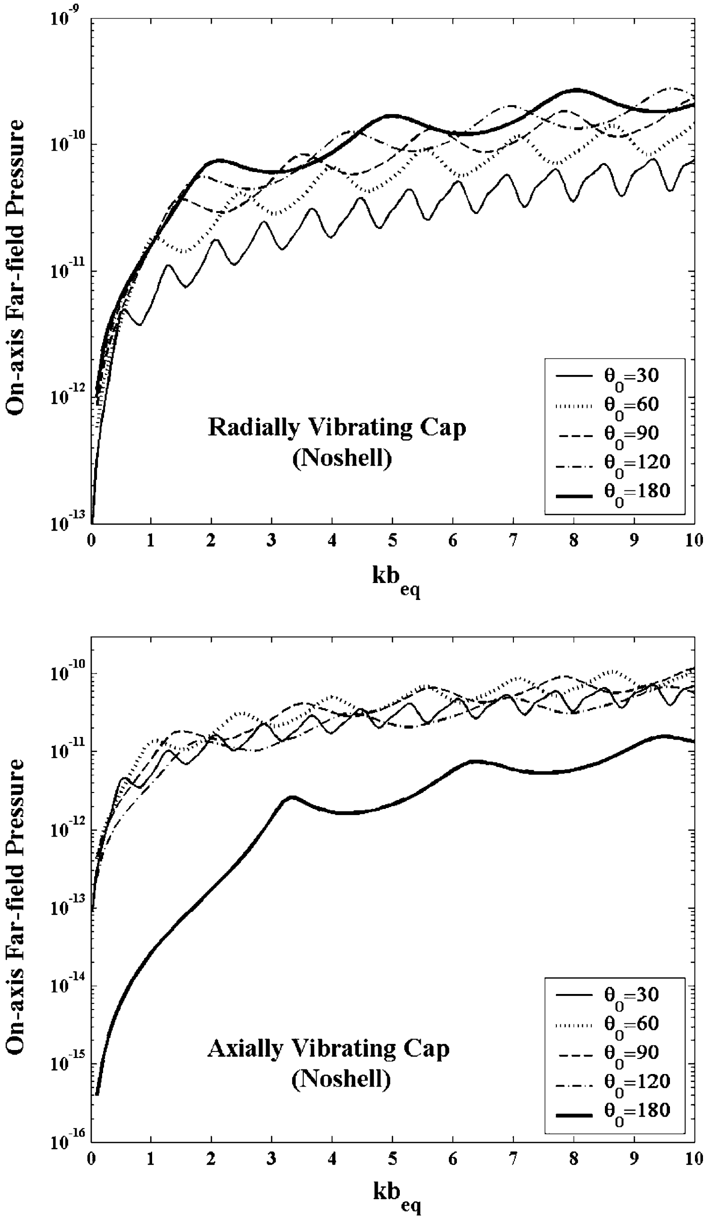

Fig. 3. The change in the on-axis far-field pressure magnitude with the nondimensional frequency for the radially/axially vibrating piston positioned in the center of the fluid sphere for selected the cap angles.

sional frequency is increased, the far-field pressure curves seem to oscillate about and approach a steady value. Encapsulating the source by the elastic shell causes a noticeable increase in the overall amplitude of the resonant oscillations that build up in the far-field pressure curves. Decreasing the cap angle leads to a general increase in the number of resonant peaks. Moreover, increasing the cap angle for the radially (axially) vibrating piston instigates an overall increase (decrease) in pressure amplitudes.

Next, in order to determine the focal points associated with the shell-encapsulated source (Thompson, 1973; Hasheminejad and Azarpeyvand, in press), we plot in Figs. 4 and 5 the form function amplitude $10\log f_\infty(\omega, r_0)$ versus the source eccentricity r_0/b at the nondimensional frequencies corresponding to the first and second peak frequencies that appear in Fig. 2 for selected cap angles $\theta_0 = 30^\circ$, 60°, 180° (see Table 2). Here, we remind that the form functions are normalization with respect to the case when the source is positioned exactly at the center of the shell. Consequently, except in the wholly translating ($\theta_0 = 180^\circ$) source case (Fig. 5), a relative minimum is observed in the figures when the source is positioned at (near) the center of the encapsulating shell for all cap angles. Furthermore, in the latter case (i.e. $\theta_0 = 180^\circ$), the form function amplitude turns out to be negative which

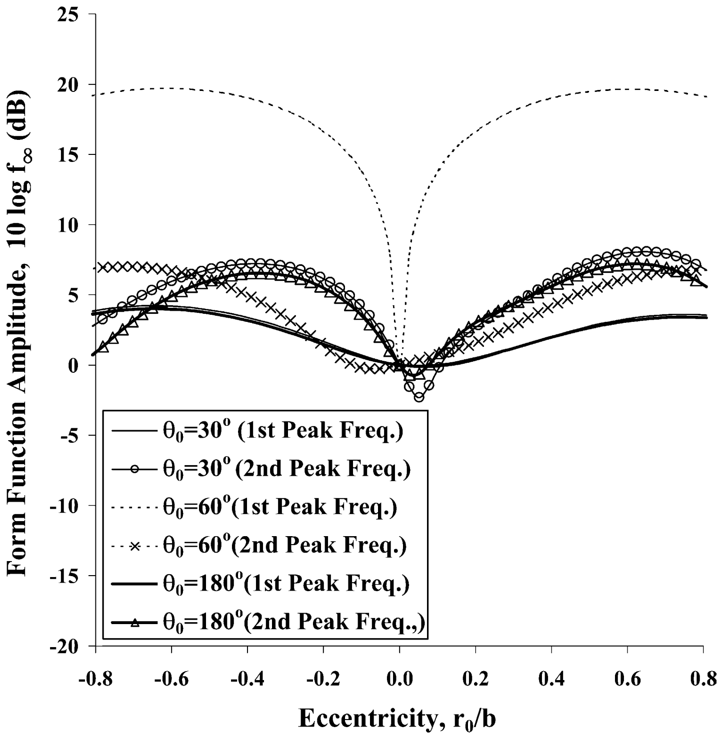

Fig. 4. The form function amplitude versus the source eccentricity at the first and second peak frequencies for the radially vibrating piston at selected cap angles.

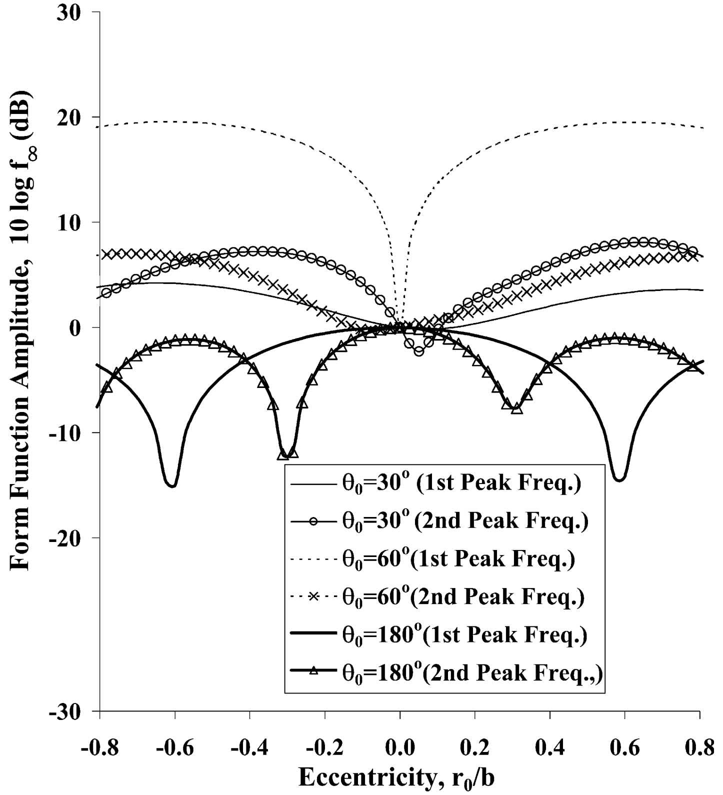

Fig. 5. The form function amplitude versus the source eccentricity at the first and second peak frequencies for the axially vibrating piston at selected cap angles.

demonstrates the adverse effect of source eccentricity on the radiated far-field pressure. The eccentricity values corresponding to the primary and secondary focal

Table 2
Nondimensional peak frequencies

Cap angle	Nondimensional frequency (kb_e)			
	Radial vibration		Axial vibration	
	First peak frequency	Second peak frequency	First peak frequency	Second peak frequency
$\theta_0 = 30^\circ$	1.13	1.93	1.13	1.93
$\theta_0 = 60^\circ$	1.70	2.20	1.70	2.20
$\theta_0 = 90^\circ$	2.40	3.10	2.40	3.10
$\theta_0 = 120^\circ$	2.93	3.80	2.93	3.83
$\theta_0 = 180^\circ$	4.37	7.50	3.46	6.95

Table 3
The primary and secondary focal points corresponding to the first and second peak frequencies of the shell-encapsulated piston

Cap angle	Focal point	Eccentricity values (r_0)			
		Radial vibration		Axial vibration	
		First peak frequency	Second peak frequency	First peak frequency	Second peak frequency
$\theta_0 = 30^\circ$	Primary	$-0.651b$	$0.630b$	$-0.651b$	$0.651b$
	Secondary	$0.730b$	$-0.370b$	$0.730b$	$-0.380b$
$\theta_0 = 60^\circ$	Primary	$-0.599b$	$-0.729b$	$-0.610b$	$-0.710b$
	Secondary	$0.599b$	$0.781b$	$0.610b$	$0.781b$
$\theta_0 = 180^\circ$	Primary	$-0.651b$	$0.625b$	$0.000b$	$0.000b$
	Secondary	$0.730b$	$-0.365b$	$0.800b$	$0.573b$

points at the first and second peak frequencies, as read from Figs. 4 and 5, are summarized in Table 3.

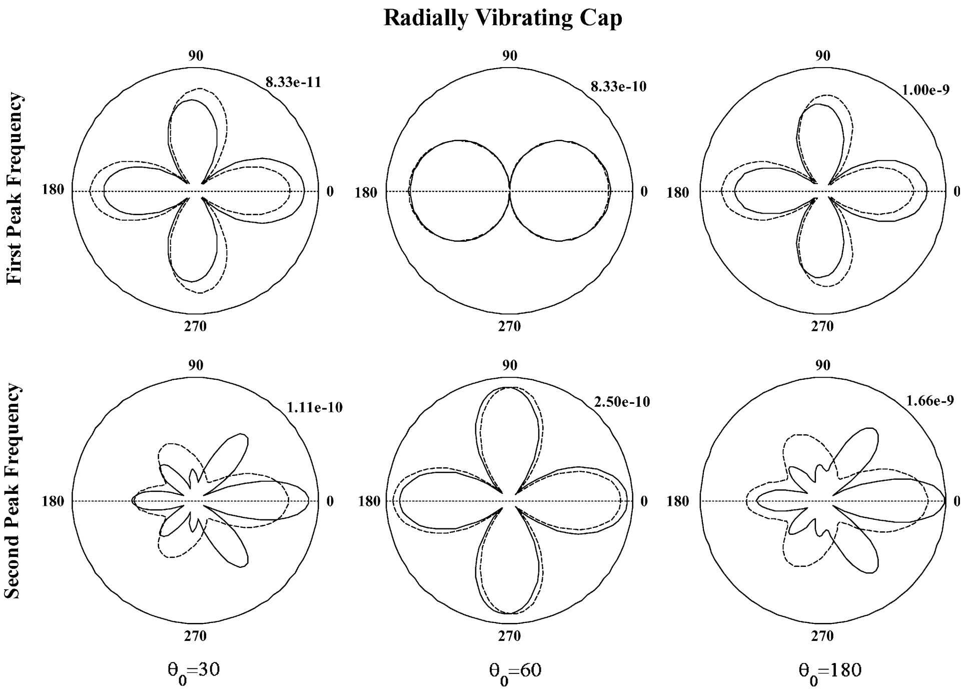

Fig. 6. The influence of cap angle on angular distribution of the radiated far-field pressure at the primary and secondary focal points corresponding to the first and second peak frequencies of the shell-encapsulated radially vibrating piston (the solid/dashed line curves correspond to the primary/secondary focal points).

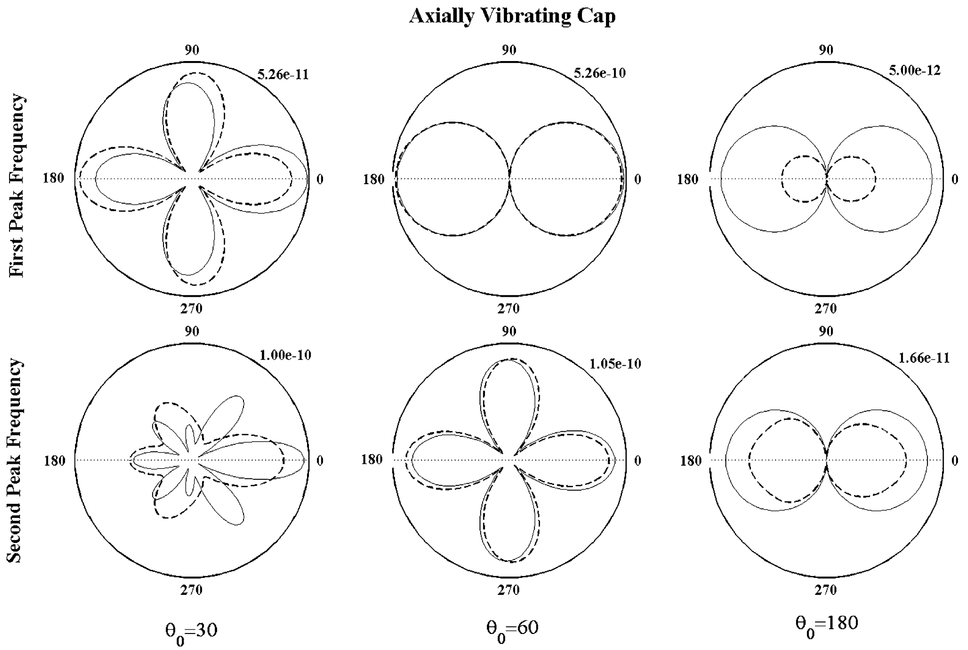

Fig. 7. The influence of cap angle on angular distribution of the radiated far-field pressure at the primary and secondary focal points corresponding to the first and second peak frequencies of the shell-encapsulated axially vibrating piston (the solid/dashed line curves correspond to the primary/secondary focal points).

Figs. 6 and 7 display the influence of cap angle on angular distribution of the radiated far-field pressure at the primary and secondary focal points corresponding to the first and second peak frequencies of the shell-encapsulated piston (see Table 3). The solid (dashed) line curves correspond to the primary (secondary) focal points. It is very interesting to study the change in directionality of the radiated waves as the cap angle is varied. In the radially vibrating cap situation (Fig. 6), we first observe a noticeable increase in the far-field pressure magnitude (directionality) as the cap angle is increased to $\theta_0 = 180^\circ$. Accordingly, the most efficient sound projection characteristics (i.e. the highest far-field pressure directivity and amplitude) for the radially vibrating cap occur for the wholly pulsating source ($\theta_0 = 180^\circ$). The $\theta_0 = 60^\circ$ case is perhaps the least favourable situation, as it exhibits a relatively poor directionality and low amplitude. Furthermore, in this case, the pressure patterns corresponding to the first and second focal points almost coincide. Similar comments can be made for the axially vibrating piston problem (Fig. 7). Here, in contrast to the radially vibrating cap case, there is an appreciable increase in the far-field pressure directionality as the cap angle is decreased to $\theta_0 = 30^\circ$. Accordingly, the most efficient sound projection characteristics for the axially vibrating cap happen for the partially pulsating source ($\theta_0 = 30^\circ$). The $\theta_0 = 180^\circ$

case is the worst situation, as it exhibits a poor directionality and very low pressure amplitude.

Finally, to check overall validity of the work, we first used our code to compute the normalized average radiation impedance load per unit area on the vibrating

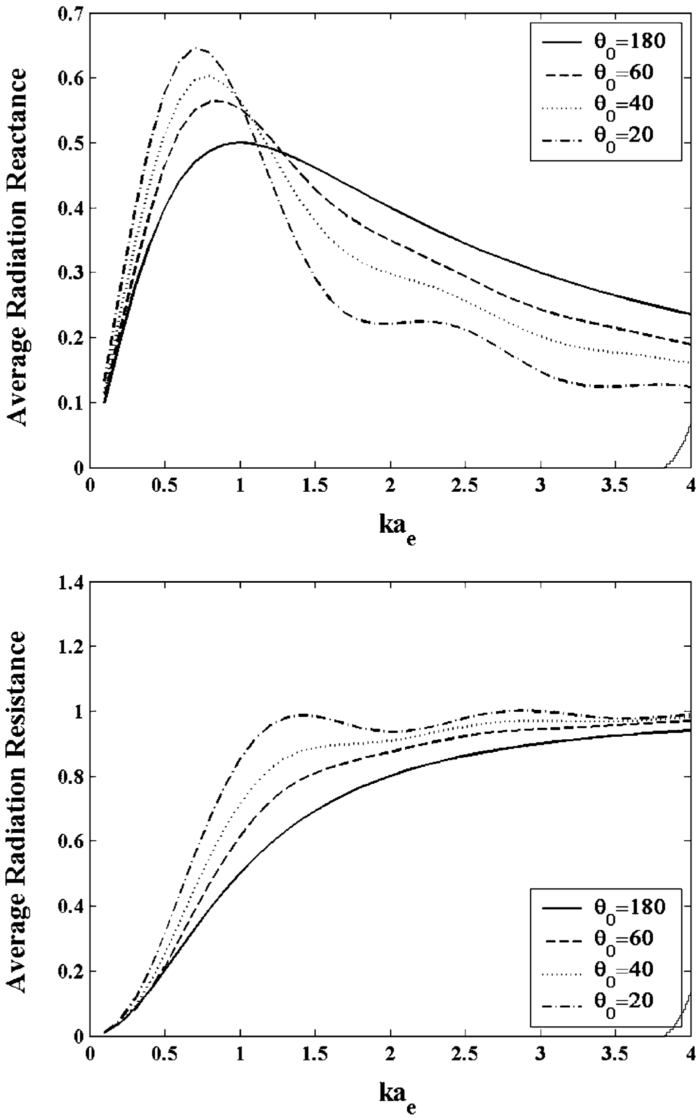

Fig. 8. Acoustic radiation impedance components for a baffled pulsating spherical cap, suspended inside a water-filled (very) light and thin spherical shell immersed in water, as a function of kb_e ($h \approx 0.0001b$, $\rho_s = \rho = \rho^* \approx 1$ g/cm^3).

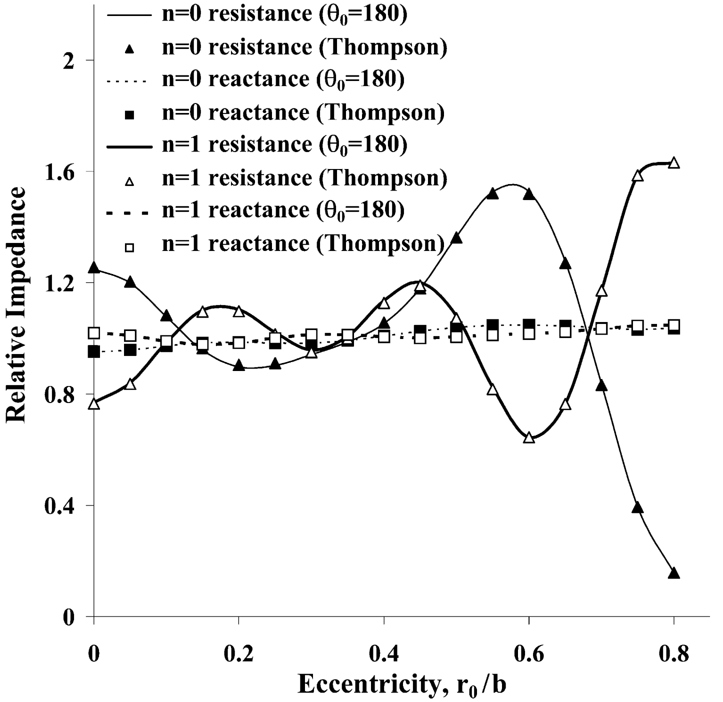

Fig. 9. The resistive and the reactive components of the relative acoustic radiation impedance for a full radially/axially vibrating cap ($\theta_0 = 180^\circ$) suspended in a (very) light and thin spherical elastic shell filled with FC-72 and immersed in water, as a function of ka_e ($h \approx 0.0001b$, $\rho_s = \rho^* \approx 1$ g/cm^3).

piston by taking advantage of Foldy's definition of the radiated power (Thompson, 1973) for the case of an eccentric baffled radially vibrating cap suspended inside a water-filled (very) light and thin spherical shell immersed in water (i.e. we set $h \approx 0.0001b$, $\rho_s = \rho = \rho^* \approx 1$ g/cm^3). Fig. 8 shows that the corresponding radiation impedance components precisely reduce to the curves appearing in Fig. 20.4, page 308, in the classic monograph by Skudrzyk (1971). Subsequently, further verifications were made for the wholly vibrating cap ($\theta_0 = 180^\circ$) suspended inside the "very thin" shell filled with "Fluorinert" chemical FC-72 and immersed in water. Fig. 9 shows that the acoustic impedance components corresponding to the radially/axially vibrating sphere agree very well with the pulsating ($n = 0$)/oscillating ($n = 1$) mode results presented in Figs. 6 and 8 of Thompson's (1973) work. Note that each curve is normalized to its corresponding value when the source is in an unbounded medium. The latter validation can also be analytically confirmed by setting $h \approx 0$ in second of (10) which automatically leads to the pertinent boundary condition for continuity of the acoustic pressure in the non-encapsulated fluid sphere problem (i.e. $\Delta p_n \approx 0 \rightarrow p_n^{\mathrm{I}} \approx p_n^{\mathrm{II}}$) (see Thompson, 1973). The continuity of the radial velocities at the fluid interface is independently satisfied according to (17).

4. Conclusions

Acoustic radiation from a shell-encapsulated baffled spherical piston, that is undergoing time-harmonic axisymmetric radial/axial surface vibrations, is examined in an exact fashion. The solution of the problem is generated by systematically analyzing multi-scattering interaction between the source and the elastic shell. Accordingly, an exact treatment of the fluid/structure interaction that involves utilization of the appropriate wave field expansions, shell dynamic equations of motion, and pertinent boundary conditions in combination with the translational addition theorems for spherical wave functions is presented. Subsequently, the basic acoustic field quantities such as the on-axis far-field radiated sound pressure (form function) and the pressure directivity pattern are evaluated for representative values of the parameters characterizing the system. The numerical results reveal that encapsulating the source by the elastic shell causes a noticeable build up of the resonant oscillations in the far-field pressure. Furthermore, the most efficient sound projection of the radially (axially) vibrating cap occurs for the wholly pulsating (partially translating) configuration. The presented study can be of practical interest in underwater acoustic lens analysis and design.

References

Abramowitz, M., Stegun, I.A., 1965. Handbook of Mathematical Functions. National Bureau of Standards, Washington, DC.

Baier, R., 1972. Acoustic radiation impedance of caps and rings on oblate spheroidal baffles. Journal of the Acoustical Society of America 51, 1705–1716.

Belcher, E.O., 1993. Multibeam, diver-held sonar using a liquid-filled, spherical acoustic lens. In: Proc. Conf. Oceans '93, October, pp. 398–402.

Boisvert, J.E., Van Buren, A.L., 2002. Acoustic radiation impedance of rectangular pistons on prolate spheroids. Journal of the Acoustical Society of America 111, 867–874.

Bostrom, A., 1980. Multiple scattering of elastic waves by bounded obstacles. Journal of the Acoustical Society of America 67, 399–413.

Boyles, C.A., 1965. Theory of focusing plane waves by spherical liquid lenses. Journal of the Acoustical Society of America 38, 393–405.

Boyles, C.A., 1969. Radiation characteristics of spherically symmetric, perfect focusing acoustic lenses. Journal of the Acoustical Society of America 45, 351–355.

Gabrielli, P., Mercier-Finidori, M., 2001. Acoustic scattering by two spheres: multiple scattering and symmetry considerations. Journal of Sound and Vibration 241 (3), 423–439.

Gaunaurd, G.C., Huang, H., 1995. Acoustic scattering by an air-bubble near the sea surface. IEEE Journal of Oceanic Engineering 20 (4), 285–292.

Gaunaurd, G.C., Huang, H., 1996. Sound scattering by a spherical object near a hard flat bottom. IEEE Transactions on Ultrasonics, Ferroelectrics, and Frequency Control 43 (4), 690–700.

Gaunaurd, G.C., Huang, H., Strifors, H.C., 1995. Acoustic scattering by a pair of spheres. Journal of the Acoustical Society of America 98 (1), 495–507.

Greenspon, J.E., Sherman, C.H., 1964. Mutual-radiation impedance and near field pressure for pistons on a cylinder. Journal of the Acoustical Society of America 36, 149–153.

Hasheminejad, S.M., 2001. Modal acoustic on a spherical radiator in an acoustic halfspace with locally reacting boundary. Acustica-Acta Acustica 87, 443–453.

Hasheminejad, S.M., Azarpeyvand, M. Harmonic radiation from a liquid-filled spherical acoustic lens with an internal eccentric spherical source. Mechanics Research Communications, in press.

Huang, H., Gaunaurd, G.C., 1997a. Acoustic scattering of a plane wave by two spherical elastic shells above the coincidence frequency. Journal of the Acoustical Society of America 101 (5), 2659–2668.

Huang, H., Gaunaurd, G.C., 1997b. Scattering of a plane acoustic wave by a spherical elastic shell near a free surface. International Journal of Solids and Structures 34 (5), 591–602.

Ivanov, Y.A., 1970. Diffraction of Electromagnetic Waves on Two Bodies. NASA Tech. Transl. F-597.

Junger, M.C., Feit, D., 1986. Sound, Structures, and Their Interaction, second ed. MIT Press, Massachusetts.

Lease, S.A., ThompsonJr., ., W., 1991a. Use of translational addition theorems for spherical wave functions in nonaxisymmetric acoustic field problems. Journal of the Acoustical Society of America 90 (2 Pt. 1), 1155–1160.

Lease, S.A., ThompsonJr., ., W., 1991b. Nonaxisymmetric acoustic radiation from a pair of sources embedded in a fluid sphere. Journal of the Acoustical Society of America 90 (2 Pt. 1), 1161–1166.

Makarchenko, N.N., Rozhin, F.V., Tonakanov, O.S., 1989. On choosing the optimal parameters of a spherical lens. Vestnik Moskovskogo Universiteta, Seriya 3 (Fizika Astronomiya) 44 (5), 6–32.

Menton, R.T., Magrab, E.B., 1973. Farfield radiation of internally generated transient acoustic pulses transmitted through a spherical shell. Journal of the Acoustical Society of America 55 (2), 237–246.

Morse, P.M., 1981. Vibration and Sound. Acoustical Society of America through American Institute of Physics.

Pierce, A.D., 1991. Acoustics; An Introduction to its Physical Principles and Applications. American Institute of Physics, New York.

Poddubnyak, A.P., Porokhovskii, V.V., Pozdeev, V.A., Dykhta, V.V., 1985. Radiation of acoustic signal generated by an internal source from a spherical elastic shell. Soviet Journal of Applied Mechanics 21 (5), 509–513.

Roumeliotis, J.A., Kanellopoulos, J.D., 1992. Acoustic eigenfrequencies and modes in a soft-walled spherical cavity with an eccentric inner small sphere. Journal of Franklin Institute 329 (4), 727–735.

Roumeliotis, J.A., Kanellopoulos, J.D., Fikioris, J.G., 1991. Acoustic resonance frequency shifts in a spherical cavity with an eccentric inner small sphere. Journal of the Acoustical Society of America 90 (2), 1144–1148.

Sherman, C.H., 1959. Mutual radiation impedance of sources on a sphere. Journal of the Acoustical Society of America 31, 947–952.

Skudrzyk, E., 1971. The Foundations of Acoustics. Springer-Verlag, New York.

ThompsonJr., ., W., 1973. Acoustic radiation from a spherical source embedded eccentrically within a fluid sphere. Journal of the Acoustical Society of America 54 (6), 1694–1707.

ThompsonJr., ., W., 1977. Acoustic coupling between two finite-sized spherical radiators. Journal of the Acoustical Society of America 62, 8–11.

ThompsonJr., ., W., 1983. Acoustic coupling between a pulsating and an oscillating sphere. Journal of the Acoustical Society of America 74, 1050–1148.

Van Buren, A.L., 1971. Acoustic radiation impedance of caps and rings on prolate spheroids. Journal of the Acoustical Society of America 50, 1343–1356.

On the acoustic properties for 3M FC. Available from: http://www.mmm.com.